6B.5 ATMOSPHERIC MERCURY MODEL EVALUATION

Pruek Pongprueksa, Che-Jen Lin*, Li Pan, Pattaraporn Singhasuk, Thomas C. Ho, and Hsing-Wei Chu

Lamar University, Beaumont, Texas

1 INTRODUCTION

Atmospheric mercury (Hg) models can be evaluated by comparison of their simulation results with corresponding observation data. In the past decade, modelers used simple statistics to evaluate model performance (mostly atmospheric mercury concentration and wet deposition) (Bergan et al. 1999; Bergan and Rodhe 2001; Bullock 2000; Cohen et al. 2004; Ebinghaus et al. 1995; Pan et al. 2008; Shia et al. 1999) because field data were not widely accessible. Recently, more observation data become available, not limited to total gas mercury but including speciated forms (elemental, reactive gas, and particulate).

Modelers use descriptive statistics (mean, median, percentile, and standard deviation etc.) to describe the data in quantitative terms. They address correlations using Pearson's correlation coefficient, *r* (Bullock and Brehme 2002; Gbor et al. 2007; Gbor et al. 2006; Pan et al. 2007; Ryaboshapko et al. 2007a; Selin and Jacob 2008) and coefficient of determination, r^2 (Bullock Jr et al. 2007; Bullock et al. 2009; Kemball-Cook et al. 2004; Pai et al. 1997; Schmolke and Petersen 2003; Selin et al. 2008; Yarwood et al. 2003).

* *Corresponding author address:* Che-Jen Lin, Lamar University, Dept. of Civil Engineering, Beaumont, TX 77710; e-mail: Jerry.Lin@lamar.edu

Also other parameters were used to evaluate model results including percentage of data points that fit within factor of 2 (Pai et al. 1997; Petersen et al. 2001; Ryaboshapko et al. 2007a), index of agreement (Hedgecock et al. 2005; Lin and Tao 2003), as well as, bias and error terms (Bullock et al. 2009; Kemball-Cook et al. 2004; Lin and Tao 2003; Ryaboshapko et al. 2007b; Seigneur et al. 2001; Seigneur et al. 2003a; Seigneur et al. 2003b; Seigneur et al. 2004a, 2004b; Selin and Jacob 2008; Vijayaraghavan et al. 2008; Xu et al. 2000; Yarwood et al. 2003; Zagar et al. 2007).

Several graphical methods are, in addition, helpful to quantify model performance. Most common methods used by atmospheric mercury modelers include scatter plot (Bullock and Brehme 2002; Gbor et al. 2007; Gbor et al. 2006; Han et al. 2008; Kemball-Cook et al. 2004; Lin et al. 2007; Lin and Tao 2003; Pai et al. 1997; Pai et al. 1999; Petersen et al. 2001; Pongprueksa et al. 2008; Schmolke and Petersen 2003; Seigneur et al. 2001; Seigneur et al. 2003a; Seigneur et al. 2003b; Seigneur et al. 2004a, 2004b; Vijayaraghavan et al. 2008; Yarwood et al. 2003; Zagar et al. 2007), time series plot (Dastoor et al. 2008; Dastoor and Larocque 2004; Gbor et al. 2007; Gbor et al. 2006; Hedgecock et al. 2005; Petersen et al. 2001; Petersen et al. 1995; Ryaboshapko et al. 2007a; Selin et al. 2007; Strode et al. 2008), and box plot (Dastoor et al. 2008; Lin et al. 2007; Pongprueksa et al. 2008; Schmolke and Petersen 2003). Other illustration methods such as range plot with capped spikes (Cohen et al. 2004; Shia et al. 1999) has also been used by some modelers but not as extensively.

In this study, we select statistical and graphical methods to evaluate atmospheric mercury models based on model inter-comparability and ease of use. The methods include performance metrics, scatter plot, Taylor's plot, and parallel coordinates plot.

2 DATA FOR EVALUATION

2.1 Observation Data

Two observation datasets for atmospheric mercury model evaluation in North America include the Canadian Atmospheric Mercury Measurement Network (CAMNet) for measurement of total gaseous mercury (TGM) concentration and the Mercury Deposition Network (MDN) for measurement of precipitation, aqueous mercury concentration, and mercury wet deposition. The CAMNet was established by the Environment Canada in 1996 to monitor one-hour sample integration of TGM concentrations. An automatic analyzer called Tekran 2537A is used to measure TGM by cold vapour atomic fluorescence. Some of the sites co-locate with the MDN network and report weekly mercury in precipitation. The CAMNet data is available through a database called NAtChem (2009a).

The MDN network is a part of the U.S. National Atmospheric Deposition Program (NADP). The network was launched in 1995 to measure wet deposition of mercury. Precipitations are collected automatically by a modified precipitation gauge, Aerochem Metrics model 301. The collected precipitations are shipped to the Hg Analytical Laboratory (HAL) at Frontier Geosciences in Seattle, WA for measurements of mercury concentrations using cold vapor atomic fluorescence. The MDN data can be obtained from the NADP's server (2009b).

Figure 1 shows a map of CAMNet and MDN sites both in 2001 and 2005. The map of the U.S. is broken down into four NWS (National Weather Service) regions (Eastern, Central, Southern, and Western).

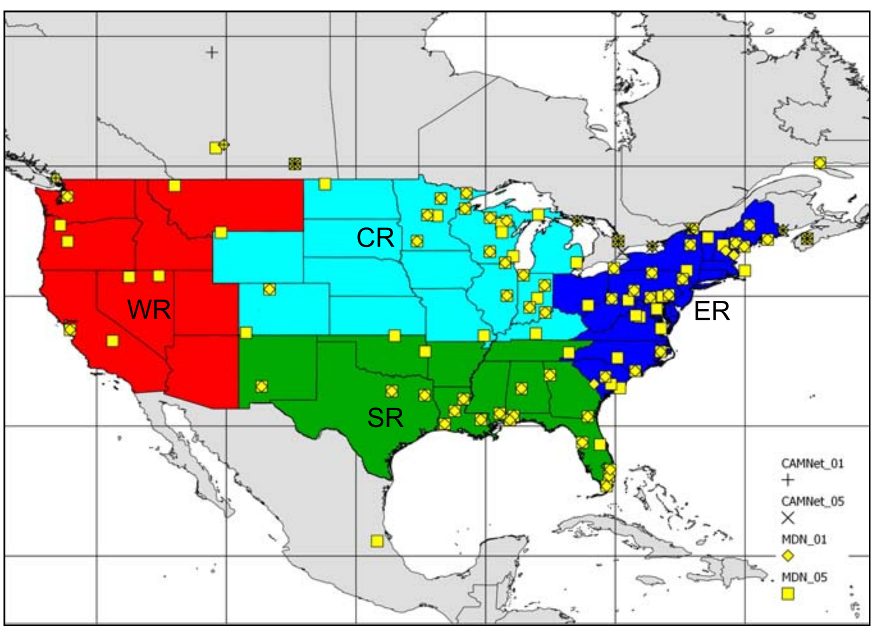

Figure 1. Map of CAMNet and MDN in 2001 and 2005 by NWS regions - Eastern (blue), Central (turquoise), Southern (green), and Western (red).

2.2 Simulation Data

Detailed model configurations for year 2001 (using CMAQ v4.6 model and the U.S. EPA's Intercontinental transport and Climatic effects of Air Pollutants (ICAP) domain) can be found in previous study (Lin et al. 2009). The 2001 model data were used in comparison with those of other model studies (LADCO, MSC-E, and NAMMIS). The Lake Michigan Air Directors Consortium (LADCO) study reported model evaluation of mercury deposition using a regional model, CAMx v4 (Comprehensive Air quality Model with extensions), for a 2002 annual simulation (Kemball-Cook et al. 2004; Yarwood et al. 2003). Studies by the Meteorological Synthesizing Centre East (MSC-E) reported model inter-comparisons (eight models) of mercury concentrations in air and precipitation over selected European countries in 1995 and 1999 (Ryaboshapko et al. 2007a; Ryaboshapko et al. 2007b). In the North American Mercury Model Inter-comparison Study (NAMMIS), mercury wet depositions each of which derived from three different regional-scale atmospheric mercury models were evaluated for 2001 model simulation: the Community Multiscale Air Quality (CMAQ) model, the Regional Modelling System for Aerosols and Deposition (REMSAD), and the Trace Element Analysis Model (TEAM) (Bullock et al. 2009).

For simulation of 2005, we employed simulated data of CMAQ v4.7 in the Contiguous United States (CONUS) domain to track model performance changes from 2001 simulation data (CMAQ v4.6). The detailed of CMAQ model and CONUS domain are described in earlier studies (Bullock and Brehme 2002; Pongprueksa et al. 2008). Some modifications of CMAQ v4.6 in CMAQ v4.7 include adding gaseous oxidation of elemental $Hg^{0}_{(g)}$ by $NO_{3(g)}$ and limiting to aqueous reduction of $Hg^{2+}_{(aq)}$ (not all $Hg^{2+}_{(aq)}$ species as implemented in CMAQ v4.6) by HO_2.

For model grid resolution, our previous study of comparable grid scaling (Pongprueksa et al. 2008) has suggested that mercury depositions simulated from fine grid resolution might be lower than coarse grid resolution. However, we expect to see some improvements in CMAQ v4.7 results since meteorological data have been improved by means of data assimilation (analysis nudging).

A recent statistical analysis has shown that aqueous mercury concentration trends of US from 1998 to 2005 are slightly declining. The annual concentration trend declines in the Northeast (-1.70 %/yr) and Midwest (-3.52 %/yr), but there is no trend in the Southeast (Butler et al. 2008). It should be plausible to use 2001 and 2005 annual data in evaluating different CMAQ versions. Hg wet depositions and Hg aqueous concentrations of 2005 are expected to be lower than the results of 2001.

3 EVALUATION METHODS

3.1 Statistical Procedures

Several factors need to be considered before a series of statistical procedures being used to evaluate the performance of atmospheric mercury models. These factors comprise comparative variable, location, and time. Comparative variables are variables that can be measured and available to be compared with model results. These variables include precipitation, wet deposition, gas concentration, and aqueous concentration. Location has a major impact to the model evaluation because of differences in geographical and meteorological conditions. Location can be a country, region, state, province, or individual site. Time is related to how data being collected with respect to measurement period. Typical time being used for Hg wet depositions and Hg aqueous concentrations are annual, season, month, and week (day and hour only available for the Hg gas measurement).

Recent atmospheric mercury model studies (Bullock et al. 2009; Kemball-Cook et al. 2004; Yarwood et al. 2003) reported only precipitation and Hg wet deposition. In this study, we use all available observed variables (precipitation, Hg wet deposition, Hg aqueous concentration, and Hg gas concentration), individual monitoring site (location), and annual data (time) for the model evaluation. Moreover, there is no standard statistical procedure specifically designed for atmospheric mercury model performance evaluation. Therefore, we utilize general performance metrics as shown in Table 1. Detailed discussions of these metrics are available elsewhere (Boylan and Russell 2006; Yu et al. 2006). Although other metrics (Spearman's ρ, Kendall's τ, % Factor of 2, and Index of agreement) may be used to show the nature of the data, the Pearson product-moment correlation coefficient (r) is more popular and can be used in comparison among model studies.

3.2 Graphical Procedures

3.2.1 Scatter plot

A scatter or bubble plot is a diagram using X-Y coordinates to display values for two variables for a set of data. The data are displayed as a set of points, each of which has the value of observation determining the position on the X-axis and the value of the model determining the position on the Y-axis. This plot is the most widely used in graphical visualization.

Figure 2 shows scatter plots of MDN/CAMNet and CMAQ for precipitation (a), Hg wet deposition (b), Hg aqueous concentration (c), and Hg gas concentration (d). We varied the point (bubble) sizes to indicate data measured in different time frames since some data were not observed for the entire year of 2001 (0.033 – 0.986 yr for MDN and 0.261 – 0.983 yr for CAMNet). To consider the impact of the sampling time, precipitation along with deposition and concentration are weighted by dividing or multiplying the data with monitoring period (time correction). All data points will be considered, yet at different magnitude of contribution depending upon quality of the data. By this means, the influences of data with short-term measurement could be restricted by smaller time correction without elimination of any imperfect data point. Precipitation and Hg wet deposition divided by time will return precipitation rate and Hg wet deposition rate, respectively. Hg aqueous and Hg gaseous concentrations multiplied by time can be perceived as Hg aqueous and Hg gas dosages (integral of concentration over time interval). We use linear regression with zero intercept (y = ax) to address the relationship between observations and model simulations.

In linear regression, the coefficient of determination (R^2) equals the square of correlation coefficient (r^2). However, R^2 presented in the plot is derived from the linear equation with zero intercept and does not equal r^2. Although time corrections do not significantly alter the slopes of precipitation and Hg wet deposition, this method may lead to inconclusive performance interpretation of Hg aqueous concentration which will be discussed in the discussions and conclusions section.

Table 1 Performance metrics for annual atmospheric mercury model performance evaluation for 2001 annual data

Metrics, Range	Parameters and formulae	LADCO Study		NAMMIS Study		This study (ICAP)			
		Precip.	Wet Dep.	Precip.	Wet Dep.	Precip.	Wet Dep.	$[Hg_{(aq)}]$	$CHg_{(g)}$
Data(Site) Number	n	54	52	51-63	51-63	62	62	62	10
Arithmetic Mean, (-∞,+∞)	$\bar{x} = \frac{1}{n}\sum_{i=1}^{n} x_i \mid \bar{y} = \frac{1}{n}\sum_{i=1}^{n} y_i$	996 | 986-1793*	9.56 | 15.5-32.21†	ND | ND	9.09 | 9.08-17.88†	1023 | 698*	10.29 | 8.77†	10.68 | 13.07‡	1.59 | 1.42¶
Standard Deviation, [0,+∞)	$\sigma_x = \sqrt{\frac{1}{n}\sum_{i=1}^{n}(x_i - \bar{x})^2} \mid \sigma_y = \sqrt{\frac{1}{n}\sum_{i=1}^{n}(y_i - \bar{y})^2}$	ND | ND	ND | ND	ND | ND	4.34 | 3.85-7.17†	421 | 287*	4.94 | 3.90†	5.18 | 4.02‡	0.15 | 0.06¶
Correlation Coefficient, [0,+1]	$r = \frac{\frac{1}{n}\sum_{i=1}^{n}(y_i - \bar{y})(x_i - \bar{x})}{\sigma_y \sigma_x}$	0.52-0.77	0.69-0.86	0.59-0.93	0.71-0.83	0.74	0.49	0.41	0.75
Root Mean Square Error, [0,+∞)	$RMSE = \sqrt{\frac{1}{n}\sum_{i=1}^{n}(y_i - x_i)^2}$	ND	ND	ND	ND	431*	4.75†	5.59‡	0.20¶
Mean Bias, (-∞,+∞)	$MB = \frac{1}{n}\sum_{i=1}^{n}(y_i - x_i)$	ND	ND	0.8-1.9*	-6-241§	-325*	-1.52†	2.40‡	-0.17¶
Mean Error, [0,+∞)	$ME = \frac{1}{n}\sum_{i=1}^{n}\lvert y_i - x_i \rvert$	ND	ND	6.1-15.3*	150-326§	350*	3.25†	4.16‡	0.17¶
Mean Normalized Bias, [-1,+∞)	$MNB = \frac{1}{n}\sum_{i=1}^{n}\left(\frac{y_i - x_i}{x_i}\right)$	0.03-1.05	0.68-2.56	ND	ND	-0.28	-0.05	0.32	-0.10
Mean Normalized Error, [0,+∞)	$MNE = \frac{1}{n}\sum_{i=1}^{n}\left(\frac{\lvert y_i - x_i \rvert}{x_i}\right)$	0.24-1.06	0.75-2.56	ND	ND	0.33	0.33	0.41	0.11
Normalized Mean Bias, [-1,+∞)	$NMB = \frac{\sum_{i=1}^{n}(y_i - x_i)}{\sum_{i=1}^{n} x_i}$	ND	ND	0.03-0.08	-0.05-0.96	-0.32	-0.15	0.22	-0.11
Normalized Mean Error, [0,+∞)	$NME = \frac{\sum_{i=1}^{n}\lvert y_i - x_i \rvert}{\sum_{i=1}^{n} x_i}$	ND	ND	0.25-0.62	0.60-1.30	0.34	0.32	0.39	0.11
Mean Fractional Bias, [-2,+2]	$MFB = \frac{2}{n}\sum_{i=1}^{n}\frac{(y_i - x_i)}{(y_i + x_i)}$	-0.02-0.57	0.42-1.04	ND	ND	-0.37	-0.15	0.22	-0.11
Mean Fractional Error, [0,+2]	$MFE = \frac{2}{n}\sum_{i=1}^{n}\frac{\lvert y_i - x_i \rvert}{(y_i + x_i)}$	0.24-0.59	0.54-1.04	0.32-0.64	0.62-0.93	0.41	0.36	0.34	0.11

Note: *x* = Observation, *y* = Simulation, ND = No Data, weekly average is underlined, * unit = mm, † unit = $\mu g\ m^{-2}$, ‡ unit = $ng\ L^{-1}$, ¶ unit = $ng\ m^{-3}$, § unit = $ng\ m^{-2}$

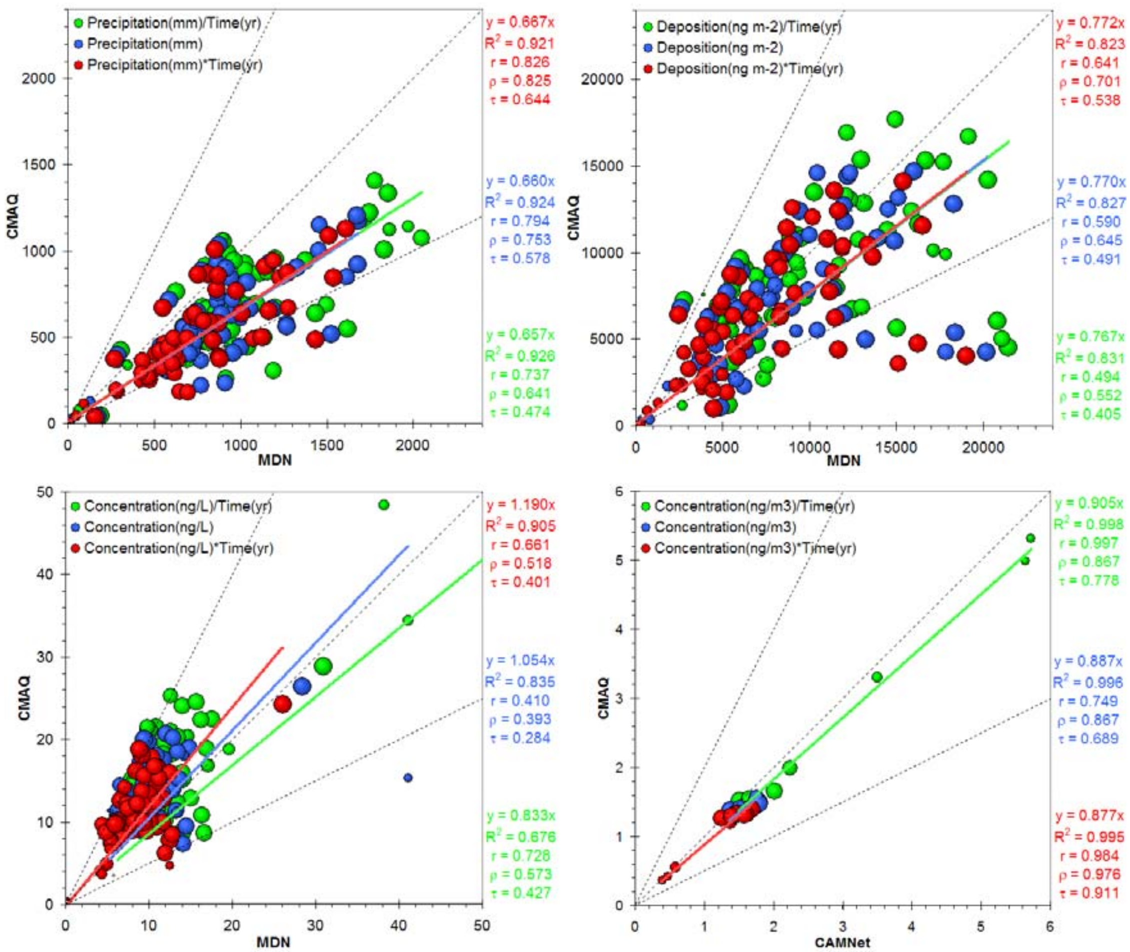

Figure 2. Scatter plots of MDN/CAMNet and CMAQ data: precipitation (a), Hg wet deposition (b), Hg aqueous concentration (c), and Hg gas concentration (d).

3.2.2 Taylor's Plot

Taylor's plot or diagram was developed by Karl E. Taylor to visualize the basic statistics used in model evaluation. The plot is a statistical diagram using polar coordinate to quantify the degree of similarity between observations and simulation results. The corresponding data are plotted into two points, one representing observation (observed or reference point) and the other representing simulation (simulated point). Radial distances from the origin to the points are proportional to the standard deviations, the angle can be transformed to the correlation coefficient, and the distance between the points gives an error term, the centered pattern Root Mean Square Error, RMSE′ (Taylor 2001). The RMSE′ is defined as:

$$RMSE' = \sqrt{RMSE^2 - (\bar{y} - \bar{x})^2} = \sqrt{\frac{1}{n}\sum_{i=1}^{n}\left[(y_i - \bar{y}) - (x_i - \bar{x})\right]^2} \quad (1)$$

the relationship between σ_x, σ_y, r, and $RMSE'$ can be arranged as:

$$RMSE'^2 = \sigma_y^2 + \sigma_x^2 - 2\sigma_y\sigma_x r \quad (2)$$

Normalizing variables in different units to be comparable in the same diagram can be done by dividing the dimensional statistics (σ_x, σ_y, and $RMSE'$) with the standard deviation of the observation dataset, σ_x, which yields non-dimensional statistics ($\sigma_x^* = \sigma_x/\sigma_x = 1$, $\sigma_y^* = \sigma_y/\sigma_x$, and $RMSE'^* = RMSE'/\sigma_x$). This keeps the correlation coefficient (r) unchanged and gives a standardized Taylor's plot. The triangle relationship between r, σ_x^*, σ_y^*, and $RMSE'^*$ is shown in Figure 3. Figure 4 shows a comparison between available data from previous model studies (MSC-E and NAMMIS) and this study (ICAP) in a standardized Taylor's plot. We do not include LADCO data owing to absence of some statistical parameters (namely standard deviation of observed and modeled data) required for constructing Taylor's plot. The ideal position for the simulation results (perfectly matching observed point) is along the radius of 1 from the origin and having angle approaching 0 (r close to 1).

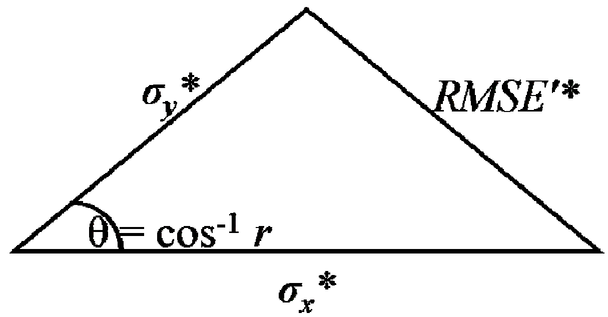

Figure 3. Triangle relationship between correlation coefficient (r), the normalized RMSE′ (RMSE′*), and the normalized standard deviation of observation and simulation (σx*, σy*).

To track performance changes caused by model versions, we compared the data from CMAQ v4.6 (ICAP_2001) and CMAQ v4.7 (CONUS_2005) using Taylor's plot as shown in Figure 5. For each variable, two points connected by an arrow are plotted; the arrow tail indicates the statistics of the original model version (CMAQ v4.6) and the arrow head represents the statistics for the new version (CMAQ v4.7). Many of the arrows in Figure 5 point away from the observed point, showing that the normalized RMSE′ between the observed and simulated data has been increased in the new model version. For precipitation, the arrow is oriented in a way that the observed and simulated variances are nearly equal in the new model, but the correlation between the two is decreased. The overall impression given by Figure 5 is that the new model has led to an overall lower model performance.

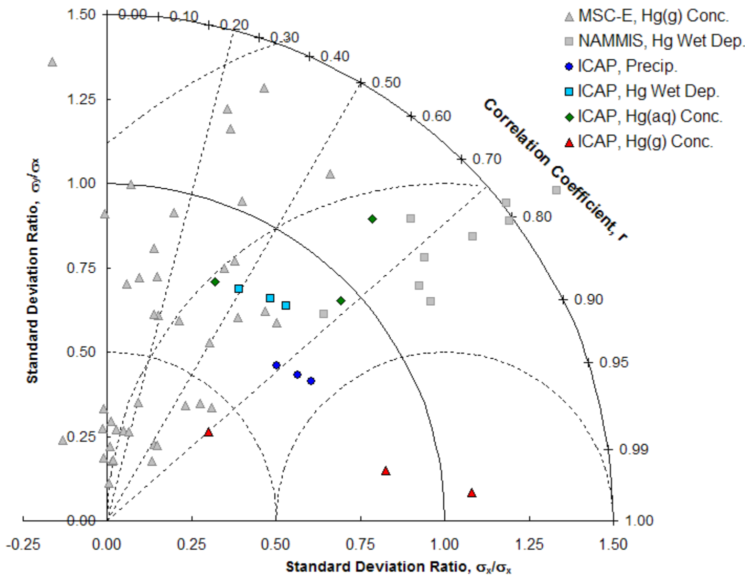

Figure 4. Taylor's plot of MSC-E, NAMMIS, and ICAP studies.

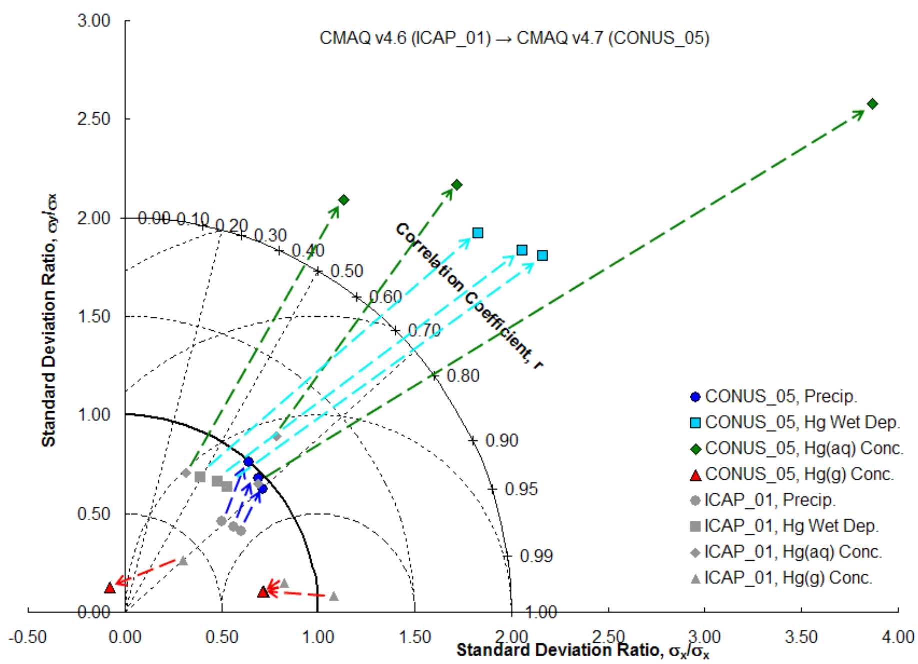

Figure 5. Taylor's Plot for Model Performance of CMAQ4.6 (ICAP_2001) and CMAQ4.7 (CONUS_2005).

3.2.3 Parallel Coordinates Plot

The parallel coordinates plot is the most straight-forward multivariate plot for presenting high-dimensional geometry and analyzing multivariate data. The vertical direction of this plot represents groups of variables, and the horizontal direction represents the parallel coordinate axes (equally spaced). Points in the same group are connected with a series of line segments with vertices on the parallel axes. The position of the vertex on an axe is determined by percentile rank of the point in each group. Variables are standardized to have zero mean and unit variance because of the widely different ranges and units. Only the median and quartiles (for both 25% and 75% points) for each group are shown. The plot does not show the outliers for each group for simplification.

To evaluate the model results of CMAQ v4.6 and CMAQ v4.7 by location, simplified parallel coordinates plots were made showing MDN and CMAQ precipitations, Hg wet depositions, and $Hg_{(aq)}$ concentrations by NWS regions (Figure 6). CMAQ v4.6 results are shown at upper section of Figure 6 and CMAQ v4.7 results are shown at the lower section. The contiguous United States is categorized into four NWS regions which include Eastern Region (ER), Central Region (CR), Southern Region (SR), and Western Region (WR) (Figure 1). Trend of discrepancies between observation and simulation data can be easily indentified by looking at the sharp slopes of the lines between MDN and CMAQ and crossed lines. We may conclude that observation and model results are likely to have less discrepancy if the lines are straight-horizontal. For CMAQ v4.6 (Figure 6-top), Southern region has discrepancy for high amount of precipitation, Hg wet deposition, and Hg concentration. Western region deviates with high precipitation and Hg wet deposition. For CMAQ v4.7 (Figure 6-bottom), the lines look less fuzzy than CMAQ v4.6 in precipitation and Hg wet deposition. The overall interpretation has led toward a general improvement in model trend except aqueous Hg concentration of Western region.

To evaluate two model versions by season, we made a similar NWS parallel coordinates plot while grouping MDN and CMAQ data into four seasons as depicted in Figure 7. Figure 7-top showing results from CMAQ v4.6 while Figure 7-bottom showing results from CMAQ v4.7. The groups of season include Winter (Dec. to Feb.), Spring (Mar. to May), Summer (Jun. to Aug.), and Fall (Sep. to Nov.). Precipitations are somewhat improved in CMAQ v4.7 (less crossed lines) but Hg wet depositions and aqueous concentrations are very similar. Both Models have similar deviation patterns in Hg wet deposition and concentration for most seasons. This may indicate that model developments in CMAQ v4.7 do not significantly alter the trend of seasonal results, especially Hg aqueous concentrations.

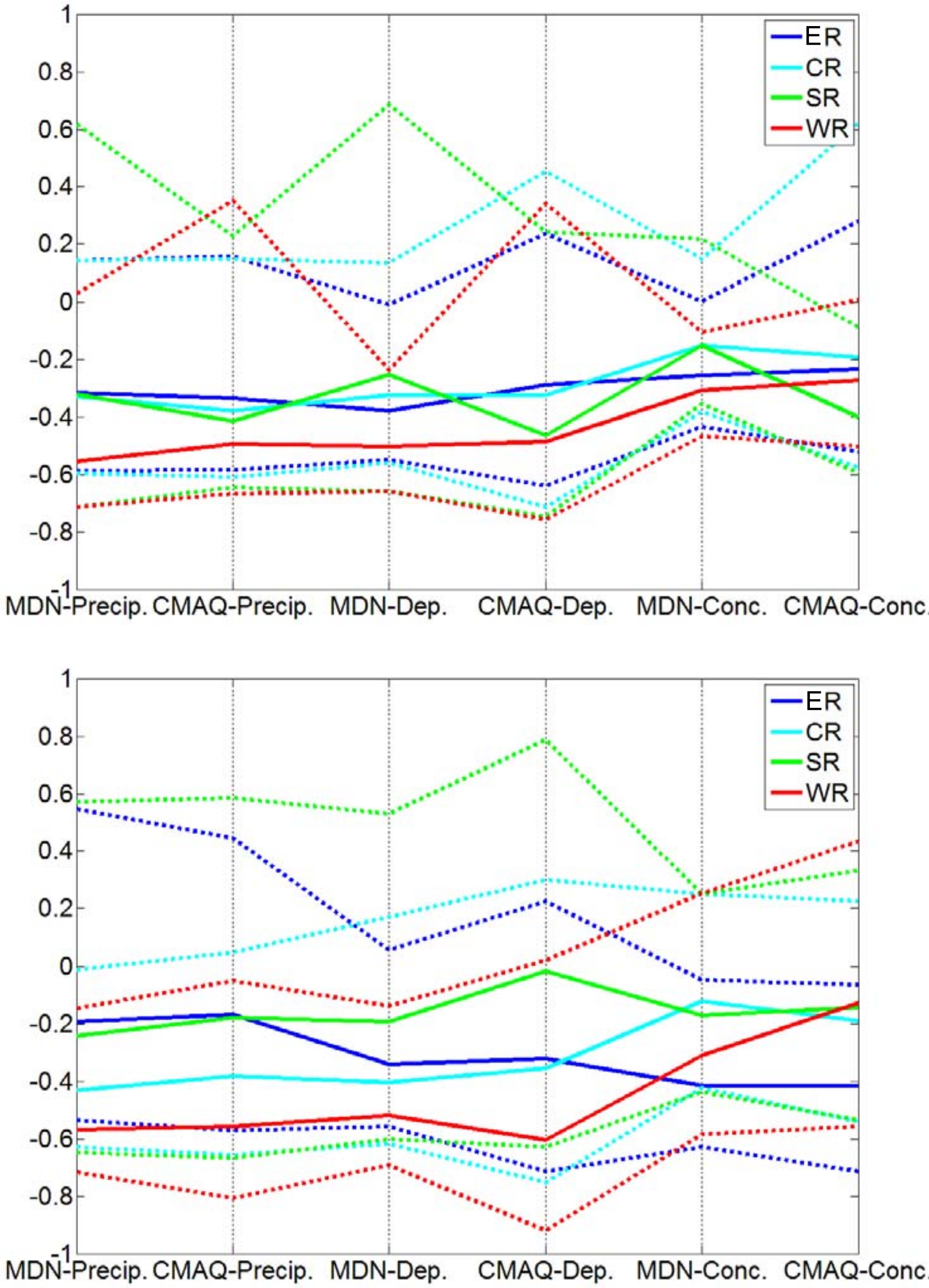

Figure 6. Parallel coordinates plots showing NWS reginal MDN and CMAQ precipitations, Hg wet depositions, and Hg(aq) concentrations in 2001 (top) and 2005 (below).

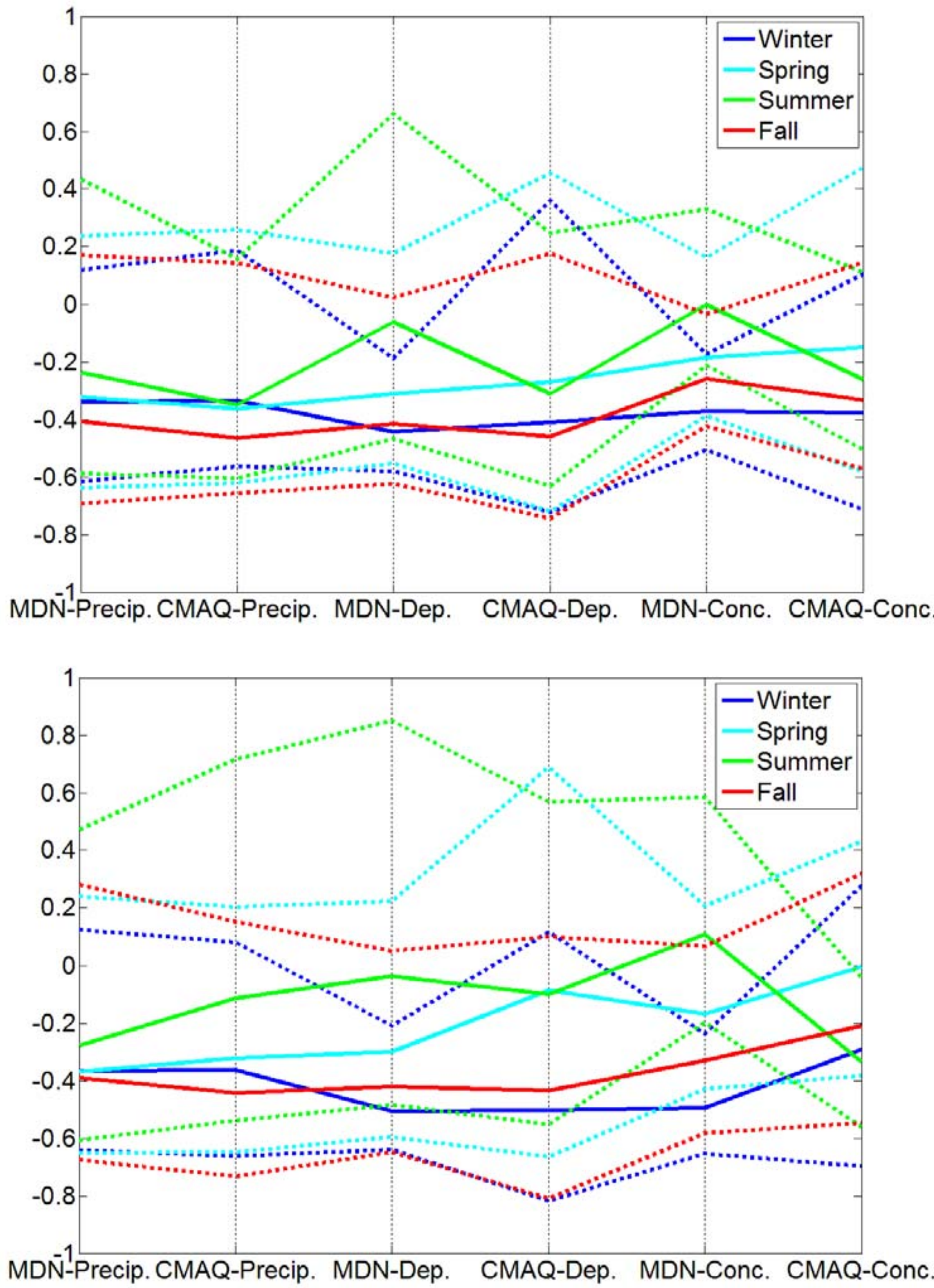

Figure 7. Parallel coordinates plots showing seasonal MDN and CMAQ precipitations, Hg wet depositions, and Hg(aq) concentrations in 2001 (top) and 2005 (below).

4 DISCUSSIONS AND CONCLUSIONS

We have used statistical and graphical methods to evaluate the performance of CMAQ-Hg v4.6 and v4.7. The techniques include performance metrics, scatter, Taylor's plot and parallel coordinates plot.

Performance metrics is a good way to quantify overall model performance in terms of errors and biases. The results can be directly compared among model studies if all the metrics are reported. However, the detailed information may not be easy for comparison.

Scatter plot is comprehensive. This method roughly shows model performance (correlation and ratio of average simulation and observation values). Bubbles in this plot can be used to illustrate completeness of observed data. Overall model performances do not change much for precipitation and Hg wet deposition when time correction is considered. This is probably due to the fact that those variables are often dependent on monitoring period (the longer period, the higher precipitaion and Hg wet deposition). To make precipitation and wet deposition time-independent, ones may normalize those data by time periods and consider the products as precipitation rate and wet deposition rate, respectively. By multiplying time correction factors, the two new variables would be converted back to the original datasets. For Hg aqueous concentration, model performance can vary from overestimation to underestimation if the time correction is applied. This may suggest that model performance of Hg aqueous concentration from this method is inconclusive and some additional data treatments (i.e. screening) may be applied in order to draw an absolute conclusion. Time correction by dividing variable is a misconception for model evaluation of precipitation rate, Hg wet deposition rate, $Hg_{(g)}$ concentration and $Hg_{(aq)}$ concentration because the products would be useless.

Taylor's plot is helpful in mercury model evaluation. This technique can also be used for tracking model performance from model developments. It is interesting to note that poor performance of CMAQ v4.7 shown in Taylor's plot is likely due to aqueous HO_2 changes. The standard deviations (as proportional to arithmetic mean) of CMAQ v4.7 results are about 3 to 4 folds of CMAQ v4.6 which are comparable to previous study (Lin et al. 2007) when aqueous HO_2 reaction is removed. The advantage of using this plot is to distinguish high correlation results; however, it is not easy to identify those with low correlation.

Parallel coordinates plot shows trend of comparison between observed data and model results. This method can suggest troubled groups (i.e. region or season) that need to be further investigated along with their model performances. It may also reveal simple model patterns or characteristics.

Using one technique to evaluate model may not give thorough understanding of model performance. The graphical methods help in model performance visualization. The statistical methods can be used in model evaluation but all available parameters should be reported. Using both statistical and graphical methods in combination provides more complete atmospheric mercury model performance evaluation.

Acknowledgements

The authors acknowledge the Canadian National Atmospheric Chemistry (NAtChem) Database and its data contributing agencies/organizations for the provision of the data for 2001 and 2005, used in this publication. The authors acknowledge the National Atmospheric Deposition Program (NADP) for precipitation and Hg wet deposition data in 2001 and 2005 used in this study. This project is supported by the Sustainable Agricultural Water Conservation (SAWC) Research Project (CSREES no. 2008-38869-01974).

References

2009a: Canadian National Atmospheric Chemistry (NATChem) Database. Environment Canada.

2009b: National Atmospheric Deposition Program (NRSP-3). NADP Program.

Bergan, T., L. Gallardo, and H. Rodhe, 1999: Mercury in the global troposphere: a three-dimensional model study. *Atmospheric Environment*, **33,** 1575-1585.

Bergan, T., and H. Rodhe, 2001: Oxidation of elemental mercury in the atmosphere; Constraints imposed by global scale modelling. *Journal of Atmospheric Chemistry*, **40,** 191-212.

Boylan, J. W., and A. G. Russell, 2006: PM and light extinction model performance metrics, goals, and criteria for three-dimensional air quality models. *Atmospheric Environment*, **40,** 4946-4959.

Bullock Jr, O. R., T. Braverman, and R. Carlos Borrego and Eberhard, 2007: Chapter 2.2 Application of the CMAQ mercury model for U.S. EPA regulatory support. *Developments in Environmental Sciences*, Elsevier, 85-95.

Bullock, O. R., 2000: Modeling assessment of transport and deposition patterns of anthropogenic mercury air emissions in the United States and Canada. *Science of the Total Environment*, **259,** 145-157.

Bullock, O. R., and K. A. Brehme, 2002: Atmospheric mercury simulation using the CMAQ model: formulation description and analysis of wet deposition results. *Atmospheric Environment*, **36,** 2135-2146.

Bullock, O. R., Jr., and Coauthors, 2009: An analysis of simulated wet deposition of mercury from the North American Mercury Model Intercomparison Study. *J. Geophys. Res.*, **114**.

Butler, T. J., M. D. Cohen, F. M. Vermeylen, G. E. Likens, D. Schmeltz, and R. S. Artz, 2008: Regional precipitation mercury trends in the eastern USA, 1998-2005: Declines in the Northeast and Midwest, no trend in the Southeast. *Atmospheric Environment*, **42,** 1582-1592.

Cohen, M., and Coauthors, 2004: Modeling the atmospheric transport and deposition of mercury to the Great Lakes. *Environmental Research*, **95,** 247-265.

Dastoor, A. P., D. Davignon, N. Theys, M. Van Roozendael, A. Steffen, and P. A. Ariya, 2008: Modeling dynamic exchange of gaseous elemental mercury at polar sunrise. *Environmental Science & Technology*, **42,** 5183-5188.

Dastoor, A. P., and Y. Larocque, 2004: Global circulation of atmospheric mercury: a modelling study. *Atmospheric Environment*, **38,** 147-161.

Ebinghaus, R., H. H. Kock, S. G. Jennings, P. McCartin, and M. J. Orren, 1995: Measurements of atmospheric mercury concentrations in Northwestern and Central Europe -- Comparison of experimental data and model results. *Atmospheric Environment*, **29,** 3333-3344.

Gbor, P. K., D. Wen, F. Meng, F. Yang, and J. J. Sloan, 2007: Modeling of mercury emission, transport and deposition in North America. *Atmospheric Environment*, **41,** 1135-1149.

Gbor, P. K., D. Wen, F. Meng, F. Yang, B. Zhang, and J. J. Sloan, 2006: Improved model for mercury emission, transport and deposition. *Atmospheric Environment*, **40,** 973-983.

Han, Y.-J., T. M. Holsen, D. C. Evers, and C. T. Driscoll, 2008: Reduced mercury deposition in New Hampshire from 1996 to 2002 due to changes in local sources. *Environmental Pollution*, **156,** 1348-1356.

Hedgecock, I. M., G. A. Trunfio, N. Pirrone, and F. Sprovieri, 2005: Mercury chemistry in the MBL: Mediterranean case and sensitivity studies using the AMCOTS (Atmospheric Mercury Chemistry over the Sea) model. *Atmospheric Environment*, **39,** 7217-7230.

Kemball-Cook, S., C. Emery, G. Yarwood, P. Karamchandani, and K. Vijayaraghavan, 2004: Improvements to the MM5-CAMx interface for wet deposition and performance evaluation for 2002 annual simulations.

Lin, C.-J., and Coauthors, 2007: Scientific uncertainties in atmospheric mercury models II: Sensitivity analysis in the CONUS domain. *Atmospheric Environment*, **41,** 6544-6560.

Lin, C. J., and Coauthors, 2009: Estimating mercury emission outflow from East Asia using CMAQ-Hg. *Atmos. Chem. Phys. Discuss.*, **9,** 21285-21315.

Lin, X., and Y. Tao, 2003: A numerical modelling study on regional mercury budget for eastern North America. *Atmospheric Chemistry and Physics*, **3,** 535-548.

Pai, P., P. Karamchandani, and C. Seigneur, 1997: Simulation of the regional atmospheric transport and fate of mercury using a comprehensive Eulerian model. *Atmospheric Environment*, **31,** 2717-2732.

Pai, P., P. Karamchandani, C. Seigneur, and M. A. Allan, 1999: Sensitivity of simulated atmospheric mercury concentrations and deposition to model input parameters. *Journal of Geophysical Research-Atmospheres*, **104,** 13855-13868.

Pan, L., and Coauthors, 2008: A regional analysis of the fate and transport of mercury in East Asia and an assessment of major uncertainties. *Atmospheric Environment*, **42,** 1144-1159.

——, 2007: Top-down estimate of mercury emissions in China using four-dimensional variational data assimilation. *Atmospheric Environment*, **41,** 2804-2819.

Petersen, G., R. Bloxam, S. Wong, J. Munthe, O. Krüger, S. R. Schmolke, and A. V. Kumar, 2001: A comprehensive Eulerian modelling framework for airborne mercury species: model development and applications in Europe. *Atmospheric Environment*, **35,** 3063-3074.

Petersen, G., Å. Iverfeldt, and J. Munthe, 1995: Atmospheric mercury species over central and Northern Europe. Model calculations and nordic air and precipitation network for 1987 and 1988. *Atmospheric Environment*, **29,** 47-67.

Pongprueksa, P., and Coauthors, 2008: Scientific uncertainties in atmospheric mercury models III: Boundary and initial conditions, model grid resolution, and Hg(II) reduction mechanism. *Atmospheric Environment*, **42,** 1828-1845.

Ryaboshapko, A., and Coauthors, 2007a: Intercomparison study of atmospheric mercury models: 1. Comparison of models with short-term measurements. *Science of The Total Environment*, **376,** 228-240.

——, 2007b: Intercomparison study of atmospheric mercury models: 2. Modelling results vs. long-term observations and comparison of country deposition budgets. *Science of The Total Environment*, **377,** 319-333.

Schmolke, S. R., and G. Petersen, 2003: A comprehensive Eulerian modeling framework for airborne mercury species: comparison of model results with data from measurement campaigns in Europe. *Atmospheric Environment*, **37,** 51-62.

Seigneur, C., P. Karamchandani, K. Lohman, K. Vijayaraghavan, and R. L. Shia, 2001: Multiscale modeling of the atmospheric fate and transport of mercury. *Journal of Geophysical Research-Atmospheres*, **106,** 27795-27809.

Seigneur, C., P. Karamchandani, K. Vijayaraghavan, K. Lohman, R.-L. Shia, and L. Levin, 2003a: On the effect of spatial resolution on atmospheric mercury modeling. *The Science of The Total Environment*, **304,** 73-81.

Seigneur, C., K. Lohman, K. Vijayaraghavan, and R.-L. Shia, 2003b: Contributions of global and regional sources to mercury deposition in New York State. *Environmental Pollution*, **123,** 365-373.

Seigneur, C., K. Vijayaraghavan, K. Lohman, P. Karamchandani, and C. Scott, 2004a: Global source attribution for mercury deposition in the United States. *Environmental Science & Technology*, **38,** 555-569.

——, 2004b: Modeling the atmospheric fate and transport of mercury over North America: power plant emission scenarios. *Fuel Processing Technology*, **85,** 441-450.

Selin, N. E., and D. J. Jacob, 2008: Seasonal and spatial patterns of mercury wet deposition in the United States: Constraints on the contribution from North American anthropogenic sources. *Atmospheric Environment*, **42,** 5193-5204.

Selin, N. E., D. J. Jacob, R. J. Park, R. M. Yantosca, S. Strode, L. Jaegle, and D. Jaffe, 2007: Chemical cycling and deposition of atmospheric mercury: Global constraints from observations. *Journal of Geophysical Research-Atmospheres*, **112,** -.

Selin, N. E., D. J. Jacob, R. M. Yantosca, S. Strode, L. Jaegle, and E. M. Sunderland, 2008: Global 3-D land-ocean-atmosphere model for mercury: Present-day versus preindustrial cycles and anthropogenic enrichment factors for deposition. *Global Biogeochemical Cycles*, **22,** -.

Shia, R. L., C. Seigneur, P. Pai, M. Ko, and N. D. Sze, 1999: Global simulation of atmospheric mercury concentrations and deposition fluxes. *Journal of Geophysical Research-Atmospheres*, **104,** 23747-23760.

Strode, S. A., L. Jaegle, D. A. Jaffe, P. C. Swartzendruber, N. E. Selin, C. Holmes, and R. M. Yantosca, 2008: Trans-Pacific transport of mercury. *Journal of Geophysical Research-Atmospheres*, **113,** -.

Taylor, K. E., 2001: Summarizing multiple aspects of model performance in a single diagram. *Journal of Geophysical Research-Atmospheres*, **106,** 7183-7192.

Vijayaraghavan, K., P. Karamchandani, C. Seigneur, R. Balmori, and S.-Y. Chen, 2008: Plume-in-grid modeling of atmospheric mercury. *J. Geophys. Res.*, **113**.

Xu, X., X. Yang, D. R. Miller, J. J. Helble, and R. J. Carley, 2000: A regional scale modeling study of atmospheric transport and transformation of mercury. I. Model development and evaluation. *Atmospheric Environment*, **34,** 4933-4944.

Yarwood, G., S. Lau, Y. Jia, P. Karamchandani, and K. Vijayaraghavan, 2003: Modeling Atmospheric Mercury Chemistry and Deposition with CAMx for a 2002 Annual Simulation.

Yu, S., B. Eder, R. Dennis, S.-H. Chu, and E. S. Schwartz, 2006: New unbiased symmetric metrics for evaluation of air quality models. *Atmospheric Science Letters*, **7,** 26-34.

Zagar, D., and Coauthors, 2007: Modelling of mercury transport and transformations in the water compartment of the Mediterranean Sea. *Marine Chemistry*, **107,** 64-88.